Low-Complexity Optimization for Near-field STAR-RIS Uplink NOMA

Seunghyun Oh, Luiggi Cantos, and Yun Hee Kim
Department of Electronics and Information Convergence Engineering
Kyung Hee University, Yongin 17104, Korea
Email: {ohioandy99, lrcantos, yheekim}@khu.ac.kr

***Abstract*—We address an extremely large (XL) simultaneously transmitting and reflecting intelligent reconfigurable surface (STAR-RIS) to the uplink non-orthogonal multiple access (NOMA) to improve the sum rate. We reformulate the sum rate maximization problem to be solvable with a low-complexity nonlinear optimization algorithm and investigate the near-field effect of the STAR-RIS on the uplink NOMA according to the STAR-RIS array configurations.**

***Index Terms*—Near-field channels, non-orthogonal multiple access, STAR-RIS, uplink**

I. Introduction

For the sixth generation (6G) wireless networks operating at a higher frequency, simultaneously transmitting and reflecting-reconfigurable intelligent surface (STAR-RIS) have attracted tremendous attention due to its capability of creating full-duplex relay channels with full coverage [1]. In particular, the STAR-RIS with the energy splitting over transmitting (T) and reflecting (R) coefficients has shown to create the synergistic effect with non-orthogonal multiple access (NOMA) [1], [2]. However, most studies have been limited to a moderate number of STAR-RIS elements under the far-field channel models.

To overcome the multiplicative fading of the STAR-RIS cascaded channels, the number of STAR-RIS elements should be large and the channels near to the STAR-RIS tend to show the near-field effects. Thus, the recent studies have investigated the near-field effects of STAR-RISs with an extremely large (XL) number of elements using a metasurface-based STAR-RIS in the downlink spatial division multiple access (SDMA) [3] and a patch-array based STAR-RIS in the downlink SDMA [4] and in the uplink NOMA [5]. In [5], a computationally efficient optimization algorithm was proposed to identify the sum rate of the XL STAR-RIS assisted uplink NOMA with the ES protocol under the quality-of-service (QoS) constraints. This paper reformulates the sum rate optimization problem in [5] without QoS constraints to be solvable with low-complexity non-linear optimization methods. The near-field effect on the uplink sum rate is also investigated according to the STAR-RIS array configurations.

II. System and Channel Models

We consider an XL-STAR-RIS assisted uplink, where a base station (BS) communicates with K users through an XL-STAR-RIS. The users in the T and R regions of the STAR-RIS are grouped as $\mathcal{K}_t$ and $\mathcal{K}_r$, respectively, with

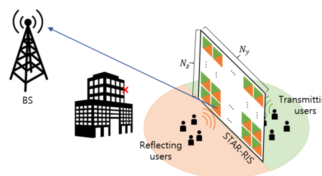

Fig. 1: System model of an XL-STAR-RIS assisted uplink.

$K = |\mathcal{K}_t| + |\mathcal{K}_r|$. The STAR-RIS consists of T coefficients $\boldsymbol{\theta}_t = [\sqrt{\beta_{t1}}e^{j\phi_{t1}}, \sqrt{\beta_{t2}}e^{j\phi_{t2}}, \cdots, \sqrt{\beta_{tN}}e^{j\phi_{tN}}]^T$ and R coefficients $\boldsymbol{\theta}_r = [\sqrt{\beta_{r1}}e^{j\phi_{r1}}, \sqrt{\beta_{r2}}e^{j\phi_{t2}}, \cdots, \sqrt{\beta_{rN}}e^{j\phi_{rN}}]^T$ subject to $\beta_{tn} \in [0,1]$, $\beta_{rn} \in [0,1]$, $\phi_{tn} \in [0, 2\pi)$, and $\phi_{rn} \in [0, 2\pi)$ for $n \in \mathcal{N} \triangleq \{1, 2, \cdots, N\}$. The coefficients are subject to $\beta_{tn} + \beta_{rn} = 1$ for $n \in \mathcal{N}$ by employing the ES protocol. The STAR-RIS is modeled by $N_y \times N_z$ configurations with uniform element spacing d, located in the yz-plane. The position of the STAR-RIS element is denoted by $\mathbf{u}^{\text{star}}_{n_y,n_z} = [0, (n_y - \frac{N_y}{2})d, (n_z - \frac{N_z}{2})d]$ for $n_y = 1, 2, \cdots, N_y$, $n_z = 1, 2, \cdots, N_z$ with $\mathbf{u}^{\text{star}}_{N_y/2, N_z/2}$ at the origin. The position of user k is given by

$$\mathbf{u}_k = [r_k \sin\vartheta_k \cos\varphi_k, r_k \sin\vartheta_k \sin\varphi_k, r_k \cos\vartheta_k] \tag{1}$$

with distance r_k, azimuth angle φ_k, and depression angle ϑ_k.

There exist no direct channels between the BS and users. The cascaded channel from user k to the BS is denoted by $\mathbf{h}_k = \mathbf{g}\text{diag}(\mathbf{v}_k)$, $k \in \mathcal{K}$, where $\mathbf{g} \in \mathbb{C}^{N\times 1}$ denotes the channel between the BS and STAR-RIS and $\mathbf{v}_k \in \mathbb{C}^{N\times 1}$ denotes the channel between the STAR-RIS and user k. With the STAR-RIS closer to the users than to the BS, $\{\mathbf{v}_k\}_{k\in\mathcal{K}}$ is modelled by a line-of-sight (LOS) channel while $\mathbf{g}$ is modeled by a non-LOS (NLoS) channel. The LOS channel is modeled by the spherical wavefront near-field channel as [6]

$$[\mathbf{v}_k]_{n_y+(n_z-1)N_y} = \sqrt{\omega_k} e^{-j\frac{2\pi}{\lambda_c}\|\mathbf{u}_k - \mathbf{u}^{\text{star}}_{n_y,n_z}\|_2} \tag{2}$$

where $\omega_k = (\frac{\lambda_c}{4\pi r_k})^2$ represents the free space path-loss with wavelength λ_c. The NLOS model of $\mathbf{g}$ is based on the geometric far-field channel with L scatters [5].

The STAR-RIS aided uplink NOMA with the ES protocol allows all users to transmit their symbols x_k at power p_k at the same time. By applying the successive interference cancellation (SIC) for the ES-NOMA signal, the signal-to-interference-and-noise ratio (SINR) of user k is given by

$$\gamma_k = \frac{p_k|\mathbf{h}_k^T\boldsymbol{\theta}_{s(k)}|^2}{\sum_{\pi(l)>\pi(k)} p_l|\mathbf{h}_l^T\boldsymbol{\theta}_{s(l)}|^2 + \sigma^2}, \tag{3}$$

where $s(k) = t$ if $k \in \mathcal{K}_t$ and $s(k) = r$ if $k \in \mathcal{K}_r$ and $\pi(k)$ denotes the SIC order of k. With the rate $R_k = \log_2(1+\gamma_k)$ of user k, the sum rate, $R_{\text{sum}} = \sum_{k=1}^{K} R_k$, is given by

$$R_{\text{sum}} = \log_2\left(1 + \sum_{k\in\mathcal{K}_t} \frac{p_k\left|\mathbf{h}_k^T\boldsymbol{\theta}_t\right|^2}{\sigma^2} + \sum_{k\in\mathcal{K}_r} \frac{p_k\left|\mathbf{h}_k^T\boldsymbol{\theta}_r\right|^2}{\sigma^2}\right). \quad (4)$$

III. Low-Complexity Sum Rate Maximization

This paper aims to maximize the sum rate with respect to STAR-RIS coefficients $\mathbf{\Theta} = [\boldsymbol{\theta}_t, \boldsymbol{\theta}_r]$ and power allocation (PA) $\mathbf{p} = [p_1, p_2, \cdots, p_K]^T$ as

$$\max_{\mathbf{\Theta}\in\mathbb{C}^{N\times 2}, \mathbf{p}\in\mathbb{R}^K} \quad R_{\text{sum}} \quad (5a)$$

$$\text{s.t.} \quad \beta_{tn} + \beta_{rn} = 1,\ \beta_{tn} \geq 0,\ \beta_{rn} \geq 0,\ \forall n, \quad (5b)$$

$$0 \leq \phi_{tn} \leq 2\pi,\ 0 \leq \phi_{rn} \leq 2\pi, \forall n, \quad (5c)$$

$$0 \leq p_k \leq P_k^{\max},\ \forall k. \quad (5d)$$

This problem can be solved by applying the algorithm developed in [5] to handle an XL STAR-RIS. Although the algorithm is more efficient than the conventional approach, it still requires a length computational time for an XL number N of STAR-RIS elements exhibiting the near-field effect. In this paper, we further investigate the method reducing the computational complexity at a trade-off in performance.

First, noting that the maximum rate is achieved with maximum PA, we write the equivalent objective function, the sum SNR with maximum power, as

$$\Gamma(\mathbf{x}) = \sum_{k\in\mathcal{K}_t} \frac{P_k^{\max}\left|\mathbf{h}_k^T\boldsymbol{\theta}_t(\mathbf{x})\right|^2}{\sigma^2} + \sum_{k\in\mathcal{K}_r} \frac{P_k^{\max}\left|\mathbf{h}_k^T\boldsymbol{\theta}_r(\mathbf{x})\right|^2}{\sigma^2}. \quad (6)$$

Here, the STAR-RIS coefficients $\boldsymbol{\theta}_t$ and $\boldsymbol{\theta}_r$ are expressed with real variables $\mathbf{x} = [\boldsymbol{\beta}^T, \tilde{\boldsymbol{\phi}}_t^T, \tilde{\boldsymbol{\phi}}_r^T]$ for $\boldsymbol{\beta} = [\beta_1, \beta_2, \cdots, \beta_N]^T$, $\tilde{\boldsymbol{\phi}}_t = [\tilde{\phi}_{t1}, \tilde{\phi}_{t2}, \cdots, \tilde{\phi}_{tN}]^T$, and $\tilde{\boldsymbol{\phi}}_r = [\tilde{\phi}_{r1}, \tilde{\phi}_{r2}, \cdots, \tilde{\phi}_{rN}]^T$ by replacing $\beta_{tn} = \beta_n$, $\beta_{rn} = 1 - \beta_n$, $\phi_{tn} = 2\pi\tilde{\phi}_{tn}$, and $\phi_{rn} = 2\pi\tilde{\phi}_{rn}$. Thus, instead of $4N$ real variables for $\boldsymbol{\theta}_t$ and $\boldsymbol{\theta}_r$, we optimize the sum SNR with $3N$ real variables as

$$\max_{0\leq\mathbf{x}\leq 1} \Gamma(\mathbf{x}). \quad (7)$$

This optimization can be solved with any nonlinear optimization method yielding a suboptimal solution. With the optimal value $\Gamma^\dagger$ of (7), the sum rate is given by $R_{\text{sum}}^\dagger = \log_2(1+\Gamma^\dagger)$.

IV. Results and Discussions

We simulate the performance when the BS and STAR-RIS are located at $[40, 30, 0]$ and $[0, 0, 0]$ in meters (m), respectively. We set $f_c = \frac{3\times 10^8}{\lambda_c} = 10$ GHz and $\mathbf{g}$ is constructed with four paths exhibiting Rayleigh fading. We set $P_k^{\max} = 23$ dBm and $\sigma^2 = -100$ dBm, with an error tolerance of $\epsilon = 10^{-3}$. User location (1) is determined with distance r_k by setting $\vartheta_k = \frac{\pi}{2}$ and $\varphi_k = 0$ for R-users and $\varphi_k = \pi$ for T-users. The distance is randomly generated in $[5, 10]$ m to observe the near-field effect of the STAR-RIS for a large N.

Fig. 2(a) shows the sum rate as the number N of STAR-RIS elements increases when $K = 8$ and $N_z = 1$. The performance of the algorithm presented in [5] is compared

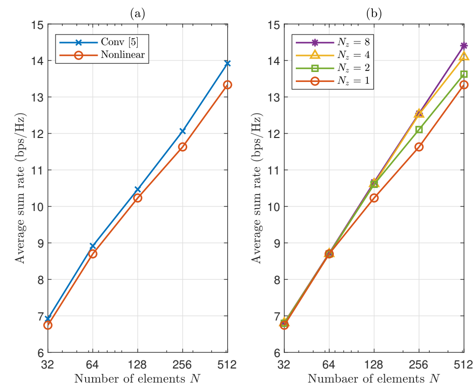

Fig. 2: Average sum rate as N increases when $K = 8$.

with that of the nonlinear optimization method, highlighting trade-offs between performance and complexity. The nonlinear optimization method exhibits a performance degradation of approximately up to 0.6 bps/Hz while reducing the computational time by 1.49 %, 5.48%, 14.06 %, 27.77 %, and 63.18 % for $N = 32$, 64, 128, 256, and 512, respectively. Therefore, nonlinear optimization can be utilized to obtain a lower bound solution for a delay-constrained system or to serve as a benchmark. The effect of the STAR-RIS configuration is also provided in Fig. 2(b) by varying N_z ($N_y = N/N_z$) for a fixed N. As N increases, the sum rate is improved but the gain is slightly reduced when N_z is smaller. The reduced gain with a smaller N_z is attributed to the near-field effect, which causes different phase responses of $\mathbf{h}_k$ with the distance of the users at the same azimuth angle. Note that the sum SNR (6) is maximized when the phases of $\mathbf{h}_k$ for $k \in \mathcal{K}_s$ are aligned for user k. Due to the spherical propagation of the near-field, the single-antenna uplink NOMA favors a planar array over a linear array for STAR-RIS configurations.

Acknowledgment

The authors would like to thank the National Research Foundation of Korea (NRF) under Grant NRF-2021R1A2C1005869 and the Institute of Information & Communications Technology Planning & Evaluation (IITP) under the Information Technology Research Center (ITRC) support program IITP-2024-2021-0-02046, with funding from the Ministry of Science and ICT (MSIT), Korea.

References

[1] M. Ahmed, et al. , "A survey on STAR-RIS: Use cases, recent advances, and future research challenges," *IEEE Internet Things J.*, vol. 10, no. 16, pp. 14 689–14 711, Aug. 2023.

[2] J. Zuo, Y. Liu, Z. Ding, L. Song, and H. V. Poor, "Joint design for simultaneously transmitting and reflecting (STAR) RIS assisted NOMA systems," *IEEE Trans. Wirel. Commun.*, vol. 22, no. 1, pp. 611–626, Jan. 2023.

[3] J. Xu, X. Mu, and Y. Liu, "Exploiting STAR-RISs in near-field communications," *IEEE Trans. Wirel. Commun.*, vol. 23, no. 3, pp. 2181–2196, Mar. 2024.

[4] H. Li, Y. Liu, X. Mu, Y. Chen, Z. Pan, and Y. C. Eldar, "Near-field beamforming for STAR-RIS networks," Jun. 2023, arXiv:2306.14587.

[5] H. A. Qureshi *et al.*, "Sum rate of extremely large STAR-RIS aided uplink NOMA," *IEEE Wirel. Commun. Lett.*, early access. [Online]. Available: https://doi.org/10.1109/LWC.2024.3401690

[6] D. Shen, L. Dai, X. Su, and S. Suo, "Multi-beam design for near-field extremely large-scale RIS-aided wireless communications," *IEEE Trans. Green Commun. Netw.*, vol. 7, no. 3, pp. 1542–1553, Sep. 2023.